Springer

KSME

Journal of Mechanical Science and Technology 27 (7) (2013) 2053~2059
www.springerlink.com/content/1738-494x
DOI 10.1007/s12206-013-0521-0

Finite element structural analysis of wind turbine gearbox considering tooth contact of internal gear system †

Jin-Rae Cho[1,2,*], Ki-Yong Jeong[1], Min-Ho Park[1], Dae-Suk Shin[2], O-Kaung Lim[1] and No-Gil Park[1]

[1]*School of Mechanical Engineering, Pusanl National University, Busan, 609-735, Korea*
[2]*Research and Development Institute of Midas IT, Gyeonggi-Do, 463-400, Korea*

(Manuscript Received March 27, 2012; Revised December 22, 2012; Accepted March 27, 2013)

Abstract

Gearbox for wind turbine must be designed to have the sufficient structural strength to sustain the extreme torque and forces transferred from rotor blades. Traditionally, the structural analysis of gearbox has been made using the simplified FEM models in which the contacts between gear teeth are replaced with the equivalent forces acting on the gear shafts, because the consideration of the detailed internal gear transmission system requires a huge number of degrees of freedom. But, the traditional method can neither accurately reflect the gear transmission forces, nor is it preferable for the dynamic analysis. In order to solve these problems, a structural analysis method considering the tooth contact of internal gear system is introduced in this paper. The actual tooth contact between a pair of gears is modeled with spring elements and the spring constants are determined through the stiffness analysis of gear teeth. The current analysis technique is justified through the comparison with the simplified gear system model and applied to the structural analysis of a 2-stage differential-type gearbox for wind turbine.

Keywords: Wind turbine gearbox; Structural analysis; FEM model considering tooth contact; Tooth stiffness coefficient; Extreme load; Equivalent stress; Shaft misalignment

1. Introduction

As natural gas and oil are getting exhausted, the demand of renewable energies such as solar-, wind- and hydro-powers and fuel cell is increasing all over the world [1]. Among them, wind power draws the intensive attention thanks to its potential to generate a huge amount of electricity from plenty of winds around us. Wind energy is transformed into electricity by wind turbine which is composed of rotor blades, step-up gear system, generator, nacelle and tower [2-4]. The step-up gear system is introduced between rotor blades and generator because the rotation number of rotor blades is extremely low to operate the generator. It is installed within a specially designed gearbox case which is in turn assembled to the nacelle [4]. Here, the gearbox is meant by a structural system composed of gears, shafts and case.

Wind turbine is not only subject to various unexpected wind loadings like a gust of wind, but it also experiences various operation conditions such as emergency stop and start up [4-6]. As a result, the resulting dangerous torque and forces generated by rotor blades are delivered directly to the step-up gear transmission system, which may result in the structural failure of not only gearbox case but also the internal gear system unless the gearbox case has the sufficient structural strength. In this context, the structural design and evaluation of gearbox becomes an important task in the development of high-durable wind turbine [7], and this task is made based upon the extreme torques and forces which are specified for a number of wind loading and operation conditions [4].

The wind-induced torque supplied to the step-up gear transmission system transfers to the gearbox via gear shafts, while the external forces stemming from the weight of rotor blades and the interaction between gearbox and generator act directly to the gearbox. Here, the forces acting on the gear shafts which are resulted from the tooth contact between a pair of gears can be analytically derived using the power-speed relation and the force equilibrium. Since the structural analysis using the detailed FEM model including all the components within a gearbox requires a painstaking meshing job and leads to a huge number of finite elements, the actual tooth contact has been traditionally replaced with the forces acting on the gear shafts. However, this traditional method can neither reflect the gear flexibility and the accurate gear transmission forces, nor is it recommendable for the dynamic analysis because the distributed gear mass should be lumped to the gear shaft [8].

*Corresponding author. Tel.: +82 51 510 3080, Fax.: +82 51 514 7640
E-mail address: jrcho@pusan.ac.kr
† Recommended by Associate Editor Chang-Wan Kim

According to our literature survey, Ramamurti et. al [9] used the simplest model to analyze the displacement and natural frequencies of a two-stage gearbox, in which only the gearbox case was modeled and the shaft reactions on bearings were applied to the inner surfaces of bearing fitting holes. Musial et al. [7] numerically analyzed the internal gear and bearing load reactions and internal displacements and motion of 2.5MW wind turbine gearbox. They constructed the 3D full finite element model including the detailed teeth of gears using SimPack^{TM} software. Lethé et al. [10] carried out the detailed and integrated 3D multibody simulation of the whole wind turbine using LMS Virtual Lab to numerically assess the structural stability under the extreme and unpredictable loads. They used the full gearbox model by considering the detailed gear teeth as well as the complex case geometry, bearings and gear shafts. Ooi et al. [11] applied the full gearbox model to the modal and stress analyses of portal axle.

Meanwhile, Li et al. [12] numerically investigated the dynamic behavior of a speed-increase gearbox using a 3-D finite element model. The tooth contact was modeled by the meshing stiffness and the profile and pitch errors of gear tooth, and the meshing stiffness of all stages of the gear transmission were evaluated by a 3-D contact FEM analysis. Peeters et al. [13] presented a 3-D flexible multibody dynamics model of a three-stage planetary gearbox in a wind turbine to simulate natural frequencies and model shapes. They considered the bearing flexibility and modeled the tooth contact by the gear meshing stiffness, and the spring stiffness was defined according to DIN 3990 as the normal distributed tooth force in the normal plane causing the deformation over a distance of $1\mu m$. The gear meshing stiffness between two gears was evaluated by loading one gear with the other fixed. Drew and Stone [14] presented a simplified method for determining the test gearbox damping level, for which the torsional natural frequency associated mainly with gear tooth flexure was identified using a numerical model of the test gearbox along. They modeled the tooth contact by a combination of linear spring and dashpot.

The main purpose of this paper is to introduce an effective and reliable structural analysis method using finite element method for analyzing the displacement and stress at the detailed component level within wind turbine gearbox in which not only the helical gear flexibility but the tooth contact is effectively considered. A gear up to the base circle is modeled as a 3-D linear elastic body, and the tooth contact between a pair of gears is modeled by spring elements with the spring constant equivalent to the stiffness of gear tooth which is evaluated by the finite element analysis. Using a simple gearbox example, the numerical accuracy and DOF-efficiency of the proposed analysis technique are justified from the comparison of the maximum displacement and natural frequencies and mode shapes with those of the simple and full gearbox models. As well, the present analysis method is applied to the structural analysis of three-stage 5 MW wind turbine gearbox to illustrate its successful and effective application to real complex gearbox in engineering applications.

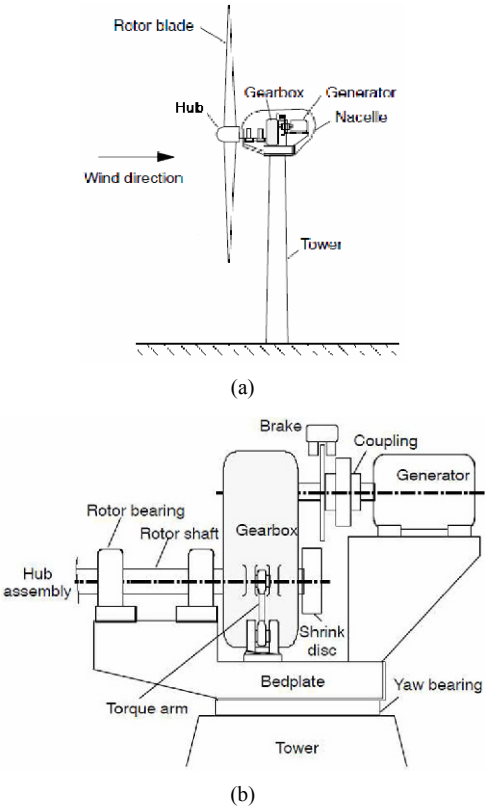

Fig. 1. Horizontal-axis wind turbine: (a) configuration; (b) detailed components.

2. Problem description

2.1 Gearbox for wind turbine

Wind turbines are classified largely into horizontal- and vertical-axis types according to the direction of rotor axis alignment [2, 3]. Fig. 1(a) depicts a horizontal-axis wind turbine (HAWT), where fan-like rotor blades, gearbox and generator which are parallel to the rotor axis are assembled using hub and nacelle. Meanwhile, the vertical-axis wind turbine (VAWT) is characterized by a circle ring-type assembly of vertical blades which is rotating with the vertical tower as the center of rotation. However, almost all of the large-capacity wind turbines are horizontal-axis type because not only it has higher structural stability but it is more advantageous for scale-up and application at sea. The role of gearbox case is to ensure the smooth tooth contact between gears, by maintaining the allowable tolerance of the radial distance between gears and by suppressing the misalignment of gear shafts [15]. In this regard, gearbox must be designed to have the sufficient structural strength against the extreme wind loading and abnormal operation conditions, not the only for preventing the structural failure.

Referring to Fig. 1(b), a pair of torque arms is attached to the gearbox case to prevent the axial rotation of gearbox, and

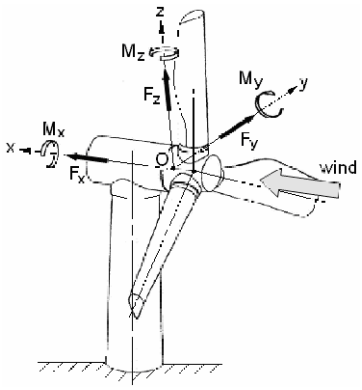

Fig. 2. Moment and force components in Cartesian coordinates.

the front rotor bearing and the rear output axis are to suppress the remaining degrees of freedom of gearbox. The configuration of gearbox and its supporting method are of course somewhat different depending on manufacturer and the power capacity. The power-capacities of current wind turbines are from several *kW*s to several *MW*s at most [5]. In general, the number of revolutions of rotor blades ranges between 10 to 20rpm while that of the output axis reaches more than 1,000rpm, implying that the step-up ratio of the wind turbine gearbox should range between 50 to 100 [4]. Wind turbine gearbox is a heavy large-scale structural system of several tons with the characteristic dimension reaching several meters at most, subject to the severe fluctuating external torques and forces. Thus, the structural and fatigue strength of wind turbine gearbox under such unstable extreme loadings is the most important requirement for the stable and accurate transmission of wind load to the generator.

2.2 External forces and moments

As mentioned above, wind turbine is subject to various unstable dynamic loads caused by gust and abnormal operating conditions like emergency stop. Since the height of wind turbine reaches several ten and hundred meters, even the normal wind produces the remarkable variation of wind velocity in the vertical direction [16]. Referring to Fig. 2, external moment and force acting on the wind turbine can be decomposed using a Cartesian coordinate system with the origin at the mass center of wind turbine and one axis aligned along the rotor axis. Here, M_x denotes the driving toque applied to the gear transmission system by the rotation of rotor blades, and M_z and F_y are owing mainly to the wind flow component inclined to the rotor axis. In addition, F_x and F_z are caused by the total axial pressure of wind and the total weight of the hub assembly while M_y is mostly produced by the difference in the wind pressure distributions of three rotor blades. Among these moment and force components, the driving torque M_x and the vertical force F_z give rise to a strong impact on the structural failure of gearbox.

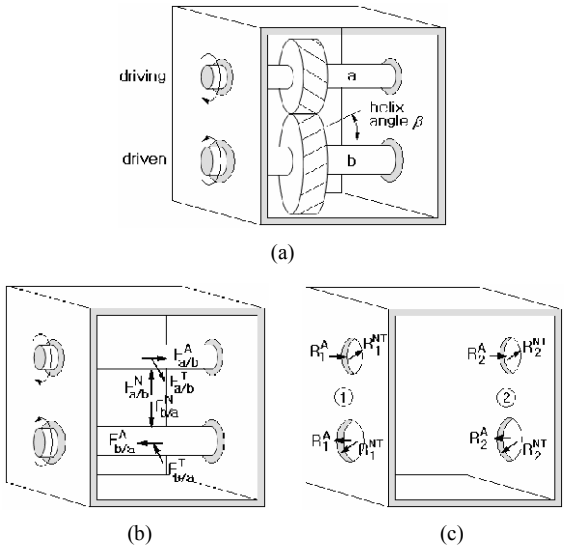

Fig. 3. Simple modeling of the tooth contact forces: (a) full model; (b) simple model 1(to the gear shaft); (c) simple model 2 (to the bearing hole).

3. Finite element structural analysis techniques

3.1 Simple and present models for wind turbine gearbox

Let us consider the traditional simple approaches to model the gear transmission force delivered through the tooth contact between a pair of gears shown in Fig. 3(a). The transmitted force $P(kg)$ can be analytically calculated by

$$P(kg)=\frac{2T}{D} \tag{1}$$

with $T(kgf\cdot m)$ and $D(m)$ being the applied torque by wind and the pitch circle of helical gear. Letting α and β be the pressure and helix angles of helical gear, the normal, tangential and axial force components of the gear transmission force P are calculated by

$$F_{a/b}^{N}=\frac{P\tan\alpha}{\cos\beta},\quad F_{a/b}^{T}=P,\quad F_{a/b}^{A}=P\tan\beta\,. \tag{2}$$

The subscript a/b indicates the gear contact force acting on gear A by gear B, and the law of action and reaction implies $F_{a/b}=-F_{b/a}$. When the gear shafts are included in the simple structural analysis model shown in Fig. 3(b), these two force components are directly applied to the gear shafts as either point loads or uniformly distributed loads. Meanwhile, when the gear shafts are further excluded, the reaction force components R^N and R^A calculated by the elementary static equilibrium are applied to the inner surface of the bearing supporting holes [9], as represented in Fig. 3(c).

The structural analysis model adopted for the current study is represented in Fig. 4, where gears are modeled as solid discs with the outer surfaces being the base circles. The contact between gear teeth is modeled using a line spring element

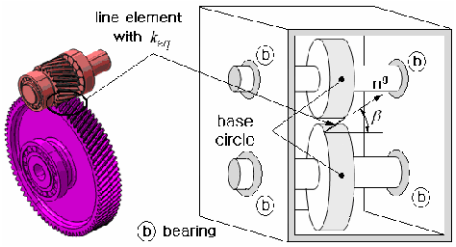

Fig. 4. Gear tooth contact modeling using spring element.

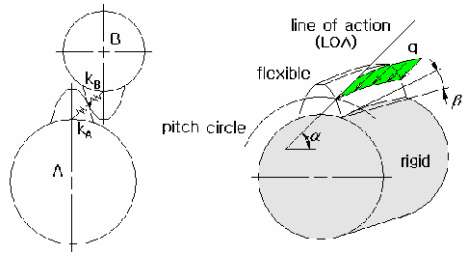

Fig. 5. FE model for evaluating the tooth stiffness coefficient.

which connects the left corner of one gear and the right corner of the other gear along the helix line. The stiffness coefficient k_{eq} (i.e., spring constant) of the line element is calculated by the finite element analysis of gear tooth described in section 3.2. By connecting two gear surfaces along the helix angle β, three components of the gear transmission force are numerically implemented.

3.2 Evaluation of the stiffness coefficient of gear tooth

Referring to Fig. 5, let us consider a contact between a pair of helical gear teeth for the sake of simple explanation. By denoting k_A and k_B be the stiffness coefficients of each tooth of helical gears A and B respectively, the equivalent stiffness coefficient of the tooth contact between a pair of helical gears with the contact ratio ℓ_c is calculated by

$$k_{eq} = \ell_c k_A k_B / \left(k_A + k_B\right). \tag{3}$$

In the current study, the stiffness coefficient of a single tooth of helical gear is evaluated by the finite element analysis. The main gear body beneath the base circle is assumed to be rigid and the uniform distributed contact force q is applied to the contact line between a pair of helical gears. The contact line is chosen at the pitch circle and the direction of the distributed load coincides with the line of action (LOA). Then, the stiffness coefficient of a single tooth of helical gear is calculated by [12]

$$k_A = \frac{qb/\cos\beta}{\delta_{LOA}} \tag{4}$$

in which b is the width of gear tooth and δ_{LOA} is the deflection of gear tooth at the pitch circle in the direction of LOA.

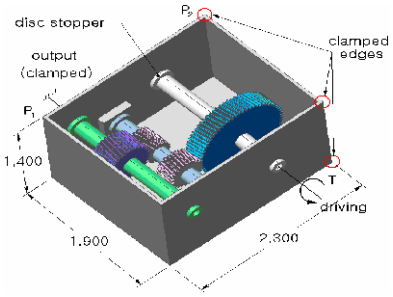

Fig. 6. A simple gear transmission system composed three gear shafts (unit: *mm*).

4. Numerical study

Two gearbox models are considered for the numerical study: a simple gearbox model for the verification of the proposed structural analysis technique and a three-stage wind turbine gearbox for the application purpose. The justification and effectiveness of the proposed method are examined by comparing the displacement and effective stress values and the total number of elements.

4.1 Numerical example

Fig. 6 shows a simple gearbox model composed of four helical gears and three shafts, where the driving shaft is subjected to an applied torque $T = 3{,}820\ kN \cdot m$ and the output shaft is not allowed to rotate. The four edges of the right plate of the gearbox with the uniform thickness t of $40\ mm$ are clamped, and the body forces of individual components are considered. The gearbox is assumed to be linearly elastic and isotropic and the density, Young's modulus and Poisson's ratio are as follows: $\rho = 6{,}920\ kg/m^3$, $E = 169.0\ GPa$ and $\nu = 0.275$ for gearbox case, $\rho = 7{,}800\ kg/m^3$, $E = 205.0\ GPa$ and $\nu = 0.29$ for idle 2 and output gears, and $\rho = 7{,}870\ kg/m^3$, $E = 200.0\ GPa$ and $\nu = 0.29$ for the remaining gears and shafts. Bearings are not included in finite element modeling by replacing them with the frictionless sliding contact between shafts with disc stoppers and the gearbox holes.

In order to compare the displacements and effective stresses, the full and simple analysis models as well as the model considering the tooth stiffness coefficient are constructed. The simple model shown in Fig. 3(b) is constructed by specifying the normal and axial forces onto the gear shafts, while the frictionless bi-directional sliding condition is specified to the tooth surfaces in contact. The finite element meshes of the full and simple models are generated with 10-node tetrahedron elements and the total numbers of elements are 1,025,647 and 64,400 respectively.

The major specifications of gear components are given in Table 1 and the contact ratios of each pair of helical gears are given as follows: 2.0508 between driving gear and idle 1 and 2.3989 idle 2 and output gear. The tooth deformations of each helical gear are obtained by the finite element analysis de-

Table 1. Major specifications of gear componenets.

Gear	Teeth number	Mod-ule	Pitch circle diameter (mm)	Tooth width (mm)	Pressure angle (deg)	Helix angle (deg)
Driving	70	16	1,1131.007	250	20	8
Idle 1	25		403.931	250		
Idle 2	18		290.163	340		7
Output	34		548.085	340		

Table 2. The tooth stiffness and equivalent stiffness coefficients.

Gear	Tooth stiffness coefficient $k\,(kN/mm)$	Contact ratio ℓ_c	Equivalent stiffness coefficient $k_{eq}\,(kN/mm)$
Driving	100.22	2.0508	105.53
Idle 1	105.77		
Idle 2	93.22	2.3989	111.18
Output	92.16		

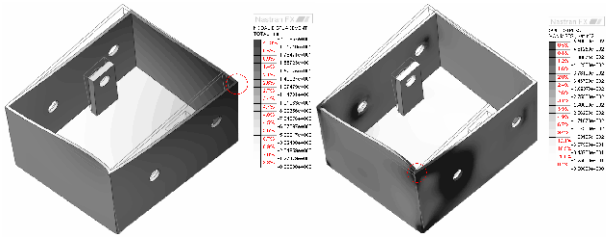

(a) (b)

Fig. 7. Numerical results of the present analysis model: (a) deformed configuration; (b) effective stress distribution.

scribed in section 3.2 and the tooth stiffness coefficients k of four helical gears which are computed using Eq. (4) are given in Table 2. The gearbox model considering the tooth stiffness coefficient is discretized with the total of 90,306 10-node tetrahedron elements.

Finite element analyses were carried out by midas NFX, commercial FEM software [17]. The displacement and the effective stress distributions of the gearbox case of the model considering the tooth stiffness coefficient are represented in Fig. 7. Referring to Fig. 6, the peak displacement is observed at point P_1 near the output gear shaft as expected, and the peak effective stress is occurred at point P_2 on the clamed edge. From the numerical results of other two simple models, it has been observed that three different analysis models lead to almost the same displacement and stress distributions. But, the maximum values are different for three models, as given in Table 3, where the values in parenthesis indicate the relative difference with respect to the values of the full model. Compared with the full model, it has been confirmed that the proposed method provides the numerical accuracy close to the full model with only the total number of elements close to the simple model.

Table 3. Comparison of the maximum displacements and effective stresses and the total numbers of elements.

Analysis model	Maximum values of FEM results		Total number of elements
	Displacement (mm)	Effective stress (N/mm^2)	
Full model	20.31	484.23	1,025,647
Simple model	20.91 (+2.95%)	542.91 (+12.14%)	64,400 (-93.72%)
Present model	20.49 (+0.89%)	493.99 (+2.02%)	90,306 (-91.20%)

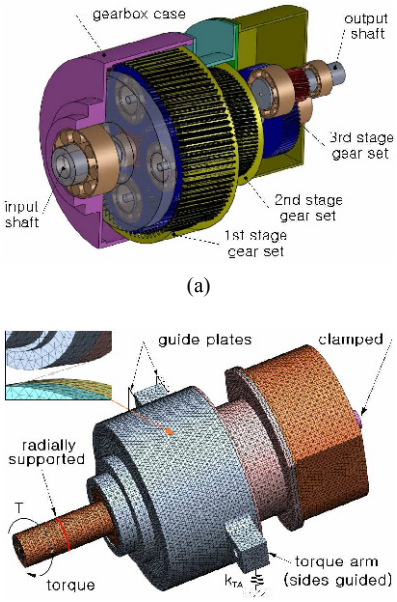

(a)

(b)

Fig. 8. A 3-stage 5 MW wind turbine gearbox: (a) internal gear system; (b) FEM model.

4.2 Application to a wind turbine gearbox

Fig. 8(a) shows a 5 MW wind turbine gearbox composed of first- and second-stage planetary gear sets and third-stage driving/driven gears. The rated input speed is 12.5rpm and the speed up ratio is 100. Each of first- and second-stage planetary gear sets consists of a fixed ring gear, four planetary gears and a sun gear. The contact angle $\alpha = 20^o$ is same for all the fourteen helical gears, but the helix angle β is set stage-wise such that $\beta = 5^o$ for the first stage, $\beta = 7^o$ for the second stage and $\beta = 8^o$ for the third stage, respectively. The density, Young's modulus and Poisson's ratio are set as follows: $\rho = 6{,}920\ kg/m^3, E = 169\ GPa$ and $\nu = 0.275$ for gearbox case, $\rho = 7{,}800\ kg/m^3$, $E = 206\ GPa$ and $\nu = 0.3$ for ring gears, and $\rho = 7{,}860\ kg/m^3$, $E = 200\ GPa$ and $\nu = 0.29$ for the remaining gears and shafts, respectively.

Referring to Fig. 8(b), the bottom surfaces of two torque arms are supported by linear springs with the spring constant k_{TA} of $300\ kN/mm$ and the side surfaces of two torque arms are constrained in the direction normal to the guide plates. The torque T corresponding to $5.0\ MW$ is applied

Table 4. The computed tooth stiffness coefficients (kN/mm).

1st-stage planetary gear set			2nd-stage planetary gear set			3rd stage gear set	
Ring	Planetary	Sun	Ring	Planetary	Sun	Driving	Driven
206.192	186.592	1537.424	109.662	92.120	93.198	100.254	105.742

Table 5. Comparison of the maximum displacements and effective stresses and the total numbers of elements.

Analysis model	Maximum values of FEM results		Total number of elements
	Displacement (mm)	Effective stress (MPa)	
Present	3.92	89.99	542,561
Simple model	4.61 (+17.6%)	100.22 (+11.37%)	394,723 (-27.25%)

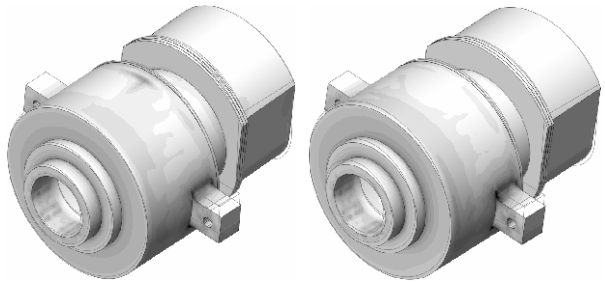

(a) (b)

Fig. 9. A 3-stage Displacement and effective stress distributions: (a) present model; (b) simple model.

to the input shaft which is constrained in the radial direction and the output shaft is constrained not to rotate. The tooth stiffness coefficients of all the helical gears are calculated according to the numerical technique described in section 3.2, and the finite element model considering the tooth contact in the present study is constructed with the total of 542,561 10-node tetrahedron elements. Meanwhile, both the normal and axial forces acting on the gear shafts of the simple model as shown in Fig. 3(b) are calculated using Eqs. (1) and (2), and those are divided by the gear widths and applied to the gear shaft surfaces as uniform distributed loads. The simple model is discretized with the total of 394,723 10-node tetrahedron elements.

The tooth stiffness coefficients obtained by the finite element analysis of a single tooth of each helical gear are given in Table 4, where sun gear in the first-stage planetary gear set shows the highest value because of its small pitch circle but large tooth width. The effective stress distributions, together with the deformed configurations, of the present and simple analysis models are comparatively represented in Fig. 9. In both models, the peak displacements occur at the tip of the right torque arm and the maximum effective stresses are observed at the upper corner of the right torque arm. As given in Table 5, the simple analysis model predicts higher displacement and effective stress by 17.6 and 11.37% than the present analysis model. The comparison between two analysis models is quite consistent with that given in Table 3 for the simple gearbox model. The present analysis model requires more finite elements than the simple analysis model, but the increase of the total element number is not significant, considering that the full analysis model requires the total of 1,570,654 elements.

5. Conclusions

A structural analysis model of wind turbine gearbox considering the tooth contact of internal gear transmission system has been introduced. The tooth stiffness coefficients of helical gears were evaluated by finite element analysis, and the tooth contact between a pair of helical gears was modeled by linearly connecting two spring elements which represent the tooth stiffness of each gear. The contact ratio between a pair of helical gears was also considered into the equivalent spring constant. Through the benchmark study using a simple gearbox model, it has been observed that the present structural analysis model provides the numerical accuracy with the relative error less than 3% with the significantly reduced total number of elements, when compared with the full analysis model considering the detailed gear teeth. The proposed model successfully applied to the structural analysis of 5 MW wind turbine gearbox, and the displacement and stress distributions of the whole wind turbine gearbox were obtained with only the total number of elements reduced by three times, compared to the total number of elements required for the full gearbox model.

Acknowledgment

This work supported by Research Program supported by the Department of Education and Technology (program name), Country Name. The financial support given to one of authors (N.G. Park) for this work by Pusan National University under the independent academic research fund (two years) is gratefully acknowledged. This work was partially supported by the Human Resources Development of the Korea Institute of Energy Technology Evaluation and Planning (KETEP) grant funded by the Korea government Ministry of Knowledge Economy (No. 20113020020010-11-1-000). The financial support for this work through World Class 300 from Ministry of Knowledge Economy of Korea is also acknowledged.

References

[1] A. D. Hansen and L. H. Hansen, Wind turbine concept market penetration over 10 years (1995-2004), *Wind Energy*, 10 (2007) 81-97.

[2] I. Paraschivoiu, *Wind turbine design with emphasis on darrieus concept*, Ecole Polytechnique de Montreal, Canada (2002).

[3] J. F. Walker and N. Jenkins, *Wind energy technology*, John Wiley & Sons, New York (1997).

[4] American gear manufacturers association, *American National Standard for Design and Specification of Gearboxes*

for Wind Turbines ANSI/AGMA/AWEA 6006-103, Virginia, USA (2003).

[5] D. C. Quarton, The evolution of wind turbine design analysis – a twenty year progress review, *Wind Energy*, 1 (1998) 5-24.

[6] M. O. L. Hansen, Aerodynamics of wind turbines, Earthscan, London, UK (2008).

[7] W. Musial, S. Butterfield and B. McNiff, Improving wind turbine gearbox reliability, *European Wind Energy Conference, NREL/CP-500-41548*, Milan, Italy (2007).

[8] H. N. Özgüven and D. R. Housner, Mathematical models used in gear dynamics – a review, *Journal of Sound and Vibration*, 121 (3) (1988) 383-411.

[9] V. Ramamurti, P. Gautam and A. Kothari, Computer-aided design of a two-stage gearbox, *Advances in Engineering Software*, 28 (1997) 73-82.

[10] G. Lethé, D. Cuyper, J. Kang, M. Furman and D. Kading, Simulating dynamics, durability and noise emission of wind turbine in a single CAE environment, *Journal of Mechanical Science and Technology*, 23 (2009) 1089-1093.

[11] J. B. Ooi, X. Wang, C. S. Tan, J. H. Ho and Y. P. Lim, Modal and stress analysis of gear train design in portal axle using finite element modeling and simulation, *Journal of Mechanical Science and Technology*, 26 (2) (2012) 575-589.

[12] R. Li, C. Yang, T. Lin, X. Chen and L. Wang, Finite element simulation of the dynamical behavior of a speed-increase gearbox, *Journal of Materials Processing Technology*, 150 (2004) 170-174.

[13] J. Peeters, D. Vandepitte and P. Sas, Flexible multibody model of a three-stage planetary gearbox in a wind turbine, *Proceedings of ISMA 2004*, 3923-3942.

[14] S. J. Drew and B. J. Stone, Torsional damping measurements for a gearbox, *Mechanical Systems and Signal Processing*, 19 (2005) 1096-1106.

[15] M. C. Garcia, M. A. Sanz-Bobi and J. del Pico, SIMAP: intelligent system for predictive maintenance allocation to the health condition monitoring of a wind turbine gearbox, *Computers in Industry*, 57 (6) (2006) 552-568.

[16] V. B. Torrance, Wind profiles over a suburban site and wind effects on a half-scale model building, *Building Science*, 7 (1) (1972) 1-12.

[17] Midas IT, On-line user's manual of midas NFX, Gyeonggi, Korea (2010).

Jin-Rae Cho received his B.S. degree in Aeronautical Engineering from Seoul National University in 1983. He then received his M.S. and Ph.D. degrees from University of Texas at Austin in 1993 and 1995, respectively. He served as an Editor of KSME International Journal and Journal of Mechanical Science and Technology. Dr. Cho is currently a vice director of the Research Institute of Midas IT Co. Ltd. Dr. Cho's current research interests include adaptive computational method, natural element method, computational tire mechanics, fluid-structure interaction, functionally graded materials, footwear biomechanics and offshore renewable energy.